

# Spectrally-efficient high-speed wireless bridge operating at 250 GHz

Cyril Renaud<sup>1\*</sup>, Luis Gonzalez-Guerrero<sup>1</sup>, Haymen Shams<sup>2</sup>, Irshaad Fatadin<sup>3</sup>, John Edward Wu<sup>1</sup>, Martyn J. Fice<sup>1</sup>, Mira Naftaly<sup>3</sup>, and Alwyn J. Seeds<sup>1</sup>.

<sup>1</sup> Department of Electronic and Electrical Engineering, University College London, Torrington Place, London, WC1E 7JE, UK

<sup>2</sup> Compound Semiconductor Applications Catapult, Regus, Falcon Dr, Cardiff Bay, Cardiff, CF10 4RU, UK

<sup>3</sup> National Physical Laboratory, Teddington, TW11 0LW, U.K

\* c.renaud@ucl.ac.uk

**Keywords:** WIRELESS BRIDGE, THZ COMMUNICATIONS, MM-WAVE COMMUNICATIONS, MICROWAVE PHOTONICS, DIGITAL SIGNAL PROCESSING.

## Abstract

A photonic wireless bridge operating at 250 GHz is presented. Using a pilot tone-assisted phase noise compensation technique, a data rate of 40 Gbit/s is achieved using 16-quadrature amplitude modulation. Furthermore, the wireless bridge is also demonstrated in a wavelength division multiplexing scenario.

## 1 Introduction

The spectrum congestion at radio frequencies (RF) is forcing telecommunication companies to seek a solution at higher frequencies. In their 2017 technology review, Ericsson highlights the importance of the W-band (75 GHz – 110 GHz) and D-band (110 GHz – 170 GHz) for near-future fixed links [1]. In that report they also mention the possibility of using even higher frequencies in a more distant future. The reason for this is clear and can be seen in Fig. 1. The windows with relatively low atmospheric attenuation at frequencies above 275 GHz are shown by cross-hatching. Beyond this frequency the spectrum is not currently regulated. Therefore, these windows can be used in their entirety for data transmission, giving an unprecedented capacity in wireless communications. Included for comparison – in grey – are the windows above 100 GHz currently allocated to fixed services. Of particular interest for long and medium range fixed applications (distances longer than 100 m) is the first unregulated window, which stretches from 275 GHz to 325 GHz. By adding to this the 252 GHz – 275 GHz frequency range, which is already allocated to fixed services, a continuous bandwidth of 68 GHz is obtained: that is more than 5 times what is currently available in the W-band and D-band. The standards for switched point-to-point links operating in this window (252 GHz – 325 GHz) have been recently defined by the IEEE 802.15.3 working group [2]. In the document, a data rate up to 100 Gbit/s is specified for applications such as: intra-device communications, close proximity communications, wireless data centres, and backhaul/fronthaul links.

For some of these applications, the best solution may be a THz wireless bridge — a THz link connecting two portions of an optical network. It is obvious, hence, that a seamless integration of the wireless transmitter with the fibred link will be an important requirement for wireless bridges. In this context, photonic generation of THz signals offers a significant

advantage over electronic generation as it directly maps the optical signal to the THz domain [3], [4]. In this paper, a photonic wireless bridge operating at 250 GHz is reported. To track the accumulated phase noise throughout the link, a pilot tone is sent together with the data-carrying signal. In the optical receiver, after signal digitization, this tone is used to coherently down-convert the signal [5]. With this technique a data rate of 40 Gbit/s is achieved using 16-quadrature amplitude modulation (QAM). Furthermore, the wireless bridge is demonstrated in an optical multi-channel configuration, where the full band from 224 GHz to 294 GHz is used.

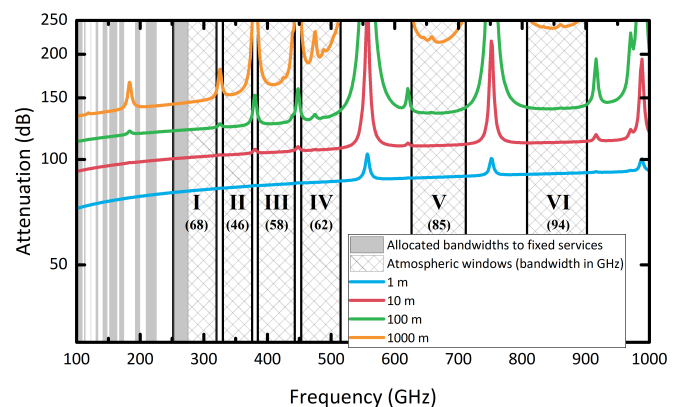


Fig. 1 Atmospheric attenuation at frequencies from 100 GHz to 1 THz (for an atmospheric pressure of 101.300 kPa, temperature of 15°C, and a water vapor density of 7.5 g/m<sup>3</sup>).

## 2. Experimental arrangement

In Fig. 2, a simplified version of the experimental arrangement used for the transmissions is shown. Three different signals were tested and transmitted with such system. The optical spectra of each of these signals is shown in Fig. 2 (b), (c) and

(d). In all the cases, the modulation employed was 16-QAM single sideband with carrier (SSB-C). The carrier was used as the reference tone for phase noise compensation. In the case of single optical channel transmission, two different bit rates were tested: 20 Gbit/s and 40 Gbit/s. For the latter rate, two 5 GBd SSB signals were multiplexed in the digital domain and mapped to opposite sidebands through appropriate digital signal processing (DSP).

For multi-channel transmission, an optical frequency comb generator (OFCG) based on a dual-drive Mach-Zehnder modulator (MZM) was used [6]. The frequency separation between lines was set to 17.5 GHz, corresponding to the maximum allowed by the OFCG (limited by the bandwidth of the electrical driver amplifiers). After selecting 5 lines with a narrow-band OBPF, these were jointly modulated with 5 GBd 16 QAM signals and then demultiplexed according to their parity (i.e., odd or even) for decorrelation.

At the central office (i.e., optical transmitter), an external cavity laser (ECL#1) emitting at a wavelength of 1551 nm was used for data modulation or, in the multi-channel transmission case, optical frequency comb generation. A single mode fiber (SMF) with a length of 10 km was used to connect the CO to the Tx remote antenna unit (RAU). The optical signal received at this unit was combined with an optical tone at a wavelength of 1549 nm (giving a frequency separation of around 250 GHz) from ECL#2, which was also used for the Rx RAU to simplify the system. After optical amplification and filtering, the two optical tones were fed into an unpackaged uni-travelling carrier photodiode (UTC-PD) by means of a lensed fiber.

For the multi-channel system, before combining the data-carrying signal with ECL#2, an OBPF was used to demultiplexed the optical channel intended for wireless transmission (i.e., the optical channels were transmitted wirelessly one at a time). Since the ECL#2 was kept at the same wavelength for all channels, the full band from 224 GHz to 294 GHz was used

Horn antennas with a gain of 25 dBi were used for both transmission and reception and placed at 0.2 m from each other. A pair of Teflon lenses with a 5 cm diameter and a back focal length of 63.2 mm were inserted between the two antennas (separation between lenses was around 10 cm) to increase the collimation of the THz beam. Such lens diameter gives a theoretical maximum gain of around 42 dB — according to  $G = (4\pi S)/\lambda^2$  where  $G$  is the gain,  $S$  is the area of the lens, and  $\lambda$  is the wavelength of the electromagnetic wave and corresponding to the diffraction-limited lossless case — which results in a total 84 dB gain for the two lens-antenna pairs. Note, however, that, due to the short transmission distance used in the experiment, a link budget calculation using the Friis formula would give unrealistic results [7].

On the Rx RAU, the signal was down-converted to a frequency of around 9 GHz with an enclosed receiver module (WR3.4MixAMC from Virginia Diodes) consisting of a  $\times 6$  multiplier, a second harmonic mixer (SHM), and an IF amplifier. After down-conversion, the IF signal was passed through two additional IF amplifiers. The resultant electrical

signal was used to drive an intensity modulator (IM) which was biased at the null point to suppress the optical carrier. After optical amplification, the signal from the IM was filtered with a narrow-band OBPF to suppress the upper sideband. Finally, after propagation through 40 km of SMF, the signal was detected and digitized in the ONU. This unit consisted of a single-ended PD, an 80 GSa/s real-time oscilloscope with a bandwidth of 36 GHz and an ECL (ECL#3). Signals of 10  $\mu$ s of duration (giving a total number of bits of around  $2 \cdot 10^5$ ) were used for bit error counting.

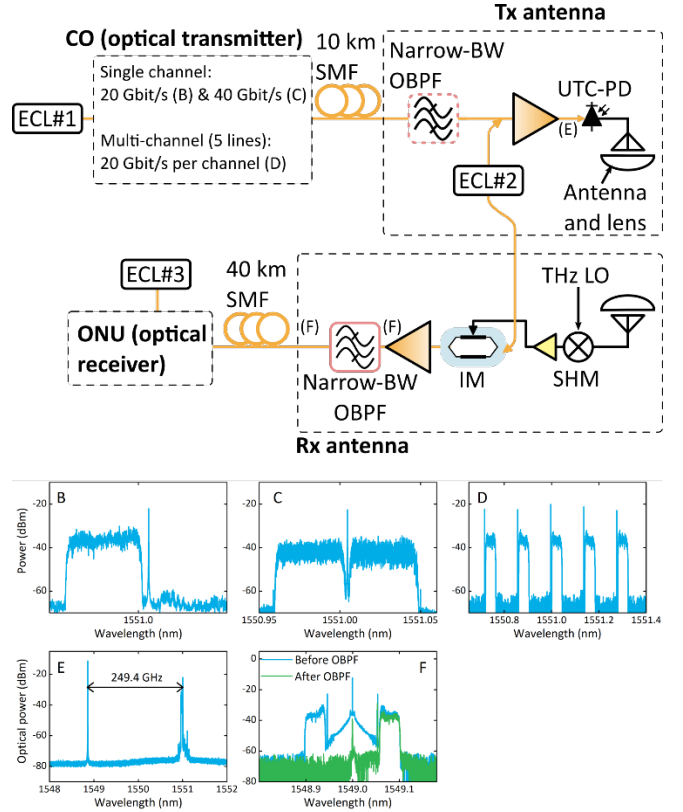


Fig 2 (a) Simplified version of the experimental arrangement used for transmissions, and optical spectra of (b) single-channel 20 Gbit/s signal, (c) 40 Gbit/s signal, (d) multi-channel transmission, (e) 20 Gbit/s signal and ECL#2 before the UTC-PD, and (f) the generated signal at the Rx RAU before (blue trace) and after (green trace) the OBPF. Note that the OBPF in the Tx RAU was only used in the multi-channel transmission.

### 3 Results

#### 3.1 Single channel

In Fig. 3, the BER of the 20 Gbit/s and 40 Gbit/s signals is plotted versus the photocurrent square ( $I_{ph}^2$ ), which is proportional to the emitted THz power. As can be seen, in both cases, a BER below the HD-FEC was obtained. From the constellation diagrams, one can see that the signal suffered from compression effects at photocurrents higher than 3 mA. Since neither changing the amplifiers nor increasing the degree of attenuation after the enclosed THz receiver corrected this (i.e., saturation effects occurred at the same value of photocurrent), these effects are likely to be caused by the THz receiver itself. Connecting directly the receiver to an ESA —

when no modulation was being sent — a power of around -40 dBm was measured for a photocurrent of 3 mA. Taking into account the power losses from the receiver, cable, and ESA this power translates into around -30 dBm of received THz power. It is important to mention that the compression point when transmitting a QAM signal (i.e., without the pilot tone) was higher. This is likely to be due to the higher peak-to-average power ratio (PAPR) of the SSB-C signal.

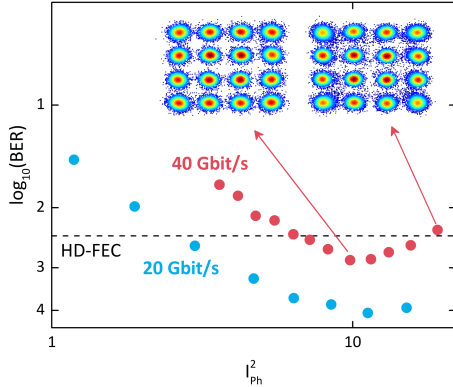


Fig. 3 BER vs. photocurrent squared for the 20 Gbit/s (blue points) and 40 Gbit/s (red points) signals.

### 3.2 Multi-channel

In Fig. 4 (a), the BER curve of each channel is plotted against  $I_{ph}^2$ . To quantify the penalty associated with the multi-channel configuration, the BER curve of a single channel was also measured. In this case, the Tx RAU OBPF was placed immediately after the optical transmitter (i.e., before the 10 km of SMF) so that only one channel propagated through the fiber. In this case, the Tx RAU EDFA was operated at maximum output power, which was measured to be 14.5 dBm. For the 5-channel transmission, on the other hand, the optimum output power from this EDFA was found to be around 7.5 dBm. A penalty of less than 2 dB at the FEC limit was found between the single- and multiple-channel transmissions.

The penalty at the FEC level of each channel with respect to the channel at 241.57 GHz (in multiple-channel operation) is plotted in Fig. 4 (b). The THz response of the system (UTC-PD and SHM) is also shown. This was measured — when no data was being sent — by connecting the enclosed receiver directly to an electrical spectrum analyser and tuning ECL#2 to scan the THz frequency. The THz LO frequency was also tuned to ensure down-conversion to the same IF (10 GHz). As can be seen, there is a strong correlation between the two curves (i.e., the higher penalty of the high-frequency channels is likely to be due to the system response roll-off at higher frequencies).

## 4 Conclusion

Wireless bridges may be crucial to realize the applications that are envisaged for THz communications. In this regard, photonic THz generation has an advantage over electronic THz generation as it directly maps the optical signal to the THz domain. In this paper, a photonic wireless bridge operating at 250 GHz is reported. For phase noise compensation, the pilot tone-assisted carrier recovery is used. With this technique a

data rate of 40 Gbit/s is achieved using 16-quadrature amplitude modulation (QAM). Furthermore, the wireless bridge is demonstrated in a wavelength division multiplexing scenario, where the full band from 224 GHz to 294 GHz is used.

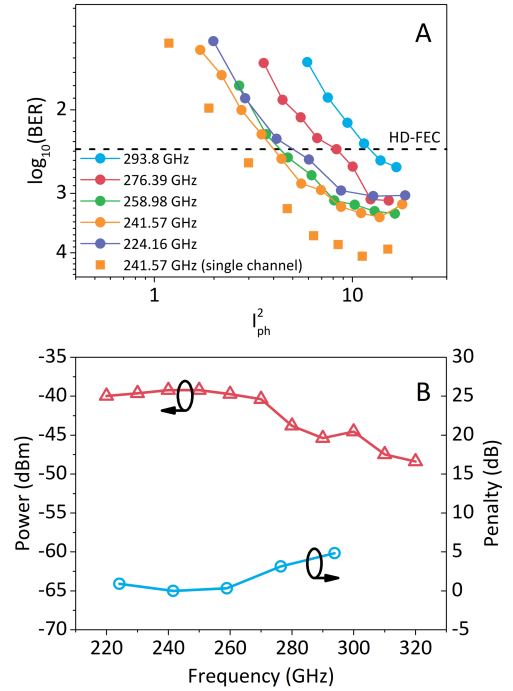


Fig. 4 (a) BER vs. photocurrent square for each channel in the multiple-channel configuration and the 241.57 GHz channel in the single-channel transmission, and (b) THz response of the system and penalty of each channel.

## 5 Acknowledgements

This work was supported by the European Union’s Horizon 2020 research and innovation programme under grant agreement 761579 (TERAPOD). This project has also received funding from the Engineering and Physical Sciences Research Council through the COALESCE (EP/P003990/1) grant.

## 6 References

- [1] J. Edstam, J. Hansryd, S. Carpenter, T. Emanuelsson, Y. Li, and H. Zirath, “Microwave backhaul evolution-reaching beyond 100GHz,” 2017.
- [2] IEEE, *IEEE Standard for High Data Rate Wireless Multi-Media Networks--Amendment 2: 100 Gb/s Wireless Switched Point-to-Point Physical Layer*, vol. 2017. 2017.
- [3] A. J. Seeds, H. Shams, M. J. Fice, and C. C. Renaud, “TeraHertz photonics for wireless communications,” *J. Light. Technol.*, vol. 33, no. 3, pp. 579–587, 2015.
- [4] T. Nagatsuma *et al.*, “Terahertz wireless communications based on photonics technologies,” *Opt. Express*, vol. 21, no. 20, p. 23736, 2013.
- [5] S. L. Jansen, I. Morita, T. C. W. Schenk, N. Takeda, and H. Tanaka, “Coherent optical 25.8-Gb/s OFDM

transmission over 4160-km SSMF,” *J. Light. Technol.*, vol. 26, no. 1, pp. 6–15, 2008.

- [6] T. Sakamoto, T. Kawanishi, and M. Izutsu, “Widely wavelength-tunable ultra-flat frequency comb generation using conventional dual-drive Mach-Zehnder modulator,” *Electron. Lett.*, vol. 43, no. 19, 2007.
- [7] H. Friis, “Simple Transmission Formula,” *Proc. IRE Waves Electrons May*, no. 1, pp. 254–256, 1946.